

Technical Report No. 32-757

A Generalized Approach to Dynamic-Stability Flight Analysis

Peter Jaffe

GPO PRICE \$ _____

CFSTI PRICE(S) \$ _____

Hard copy (HC) 1.00

Microfiche (MF) .50

ff 653 July 65

FACILITY FORM 602

<u>N65-29224</u> (ACCESSION NUMBER)	_____
<u>15</u> (PAGES)	<u>1</u> (THRU)
<u>CR 63945</u> (NASA CR OR TMX OR AD NUMBER)	<u>01</u> (CODE)
	<u>01</u> (CATEGORY)



JET PROPULSION LABORATORY
CALIFORNIA INSTITUTE OF TECHNOLOGY
PASADENA, CALIFORNIA

July 1, 1965

Technical Report No. 32-757

*A Generalized Approach to
Dynamic-Stability Flight Analysis*

Peter Jaffe

Bain Dayman, Jr.

Bain Dayman, Jr., Manager
Aerodynamic Facilities Section

**JET PROPULSION LABORATORY
CALIFORNIA INSTITUTE OF TECHNOLOGY
PASADENA, CALIFORNIA**

July 1, 1965

Copyright © 1965
Jet Propulsion Laboratory
California Institute of Technology

Prepared Under Contract No. NAS 7-100
National Aeronautics & Space Administration

CONTENTS

I. Introduction	1
II. Energy-Integral Equations	2
III. Examples	5
A. Local and Effective Constant Dynamic-Stability Coefficients	5
B. Nonlinear Aerodynamics	7
C. Nonsymmetric Bodies	8
D. Static Pitching-Moment Hysteresis	8
IV. Conclusion	10
Nomenclature	10
References	11

FIGURES

1. Sign conventions	2
2. Local and corresponding effective constant dynamic-stability curves	6
3. Typical test data	6
4. Hypothetical pitching moment due to separation hysteresis	9

ABSTRACT

29224

A general approach to the analysis of planar flight dynamic-stability investigations is presented and examples are used to discuss the approach. The foundation of the approach is the energy-integral equation which relates the energy defect during a half cycle, due to the decay, to those factors causing the decay. The equation can accommodate nonlinear aerodynamics, large oscillatory amplitudes, non-symmetric or lifting bodies, and noncontinuous or double-valued aerodynamic coefficients. Examples are presented demonstrating these applications. In addition, this Report also suggests that the usual closed-form differential solution may not be properly representing all physical mechanisms producing decay because of the continuous nature of its formulation.

Author

I. INTRODUCTION

Traditionally, in the formulation of equations used to extract dynamic-stability data from experimental free-flight information or to predict the decay, the dynamic motion is expressed as a solvable differential equation and a closed-form solution is obtained for a time interval of at least one decay measurement, a half cycle. In order to obtain this solution the theoretical model used must be the same for each differential element in the half-cycle interval. In essence this is a "microscopic" approach since the whole decay picture is built up from a single differential element. Unfortunately, it has limited application for cases of nonlinear aerodynamics, large amplitude motion, and, particularly, cases where the aerodynamic coefficients are double-valued functions of the angle of attack. Employing this differential approach, the flight equations have been developed, in detail, by Nicolaides (Ref. 1), Murphy (Ref. 2), and others. For reference, the

planar motion solution of the angle of attack, α , using this approach and assuming first-order linear aerodynamics and small angles of attack, is

$$\alpha = \alpha_0 e^{\lambda x} \cos \left\{ \left[\frac{-\rho A d}{2I} C_{m_\alpha} + \lambda^2 \right]^{1/2} X \right\} \quad (1)$$

where

$$\lambda = \frac{\rho A}{4m} \left\{ C_{D_0} - C_{L_\alpha} + \frac{md^2}{I} [C_{m_q} + C_{m_\alpha}] \right\}$$

An alternate, far more flexible method is one where the energy defect over a half cycle, as determined from the amplitude decay, is accounted for in an energy-integral equation, i.e., the energy defect due to the decay is accounted for "macroscopically." With this approach the

general nonlinear case can be considered and theoretical dynamic-stability models previously too difficult or impossible to explore can be investigated. It should be pointed out that the analytic development contained in

this Report is for planar motion; the general nonplanar case was not considered. It is felt, however, that with judicious approximations the method can be extended to include nonplanar motion.

II. ENERGY-INTEGRAL EQUATIONS

The summation of moments for a body oscillating in a plane* is

$$\sum Moments = I \ddot{\theta} = \frac{1}{2} \rho V^2 Ad \left\{ C_m + C_{m_q} \left[\frac{\dot{\theta} d}{V} \right] + C_{m_{\dot{\alpha}}} \left[\frac{\dot{\alpha} d}{V} \right] \right\} \quad (2)$$

If the independent variable is changed from time to translational distance, X , the above equation becomes

$$\theta'' \dot{X}^2 + \theta' \ddot{X} = \frac{\rho V^2 Ad}{2I} \left\{ C_m + C_{m_q} \left[\frac{\theta' \dot{X} d}{V} \right] + C_{m_{\dot{\alpha}}} \left[\frac{\alpha' \dot{X} d}{V} \right] \right\} \quad (3)$$

The angle between the velocity vector and the X axis, $[\theta - \alpha]$, is extremely small. For a very large class of problems, particularly in the supersonic regime, it is less than one-half of a degree. It is assumed, therefore, that a small angle approximation for $[\theta - \alpha]$ is valid and that

$$\dot{X} = V \cos [\theta - \alpha] = V \quad (4a)$$

$$\dot{Z} = -V \sin [\theta - \alpha] = -V [\theta - \alpha] = -\dot{X} [\theta - \alpha] \quad (4b)$$

$$\text{Force in } X \text{ direction} = -\text{drag} + mg_x \quad (4c)$$

$$\text{Force in } Z \text{ direction} = -\text{Lift} + mg_z \quad (4d)$$

Applying approximation Eq. (4a) to Eq. (3) and separating α' into θ' and $[\alpha' - \theta']$, Eq. (3) becomes

$$\theta'' = \frac{\rho Ad}{2I} \left\{ C_m + [C_{m_q} + C_{m_{\dot{\alpha}}}] \theta' d + C_{m_{\dot{\alpha}}} [\alpha' - \theta'] d \right\} - \frac{\ddot{X}}{\dot{X}^2} \theta' \quad (5)$$

The static pitching moment is a particular function of α , $C_m = C_m(\alpha)$,** while C_{m_q} and $C_{m_{\dot{\alpha}}}$ are arbitrary functions. By expanding $C_m(\alpha)$ in a Taylor series, it can be expressed as a function of θ and $[\alpha - \theta]$.

$$C_m(\alpha) = C_m(\theta) + [\alpha - \theta] \frac{dC_m(\theta)}{d\theta} + \frac{[\alpha - \theta]^2}{2!} \frac{d^2 C_m(\theta)}{d\theta^2} + \dots \quad (6)$$

Since $[\alpha - \theta]$ is extremely small, and for most physically realistic situations the higher-order derivatives of C_m remain moderate, the first two terms of the series will yield $C_m(\alpha)$ plus a negligible error. Using the first two terms then, Eq. (5) becomes

$$\theta'' = \frac{\rho Ad}{2I} \left\{ C_m(\theta) + [\alpha - \theta] \frac{dC_m(\theta)}{d\theta} + [C_{m_q} + C_{m_{\dot{\alpha}}}] \theta' + C_{m_{\dot{\alpha}}} [\alpha' - \theta'] d - \frac{2I}{\rho Ad} \frac{\ddot{X}}{\dot{X}^2} \theta' \right\} \quad (7)$$

**In this Report, the parenthesis, (), is used to denote a functional relationship only, with the exception that it may also be used for limits of integration.

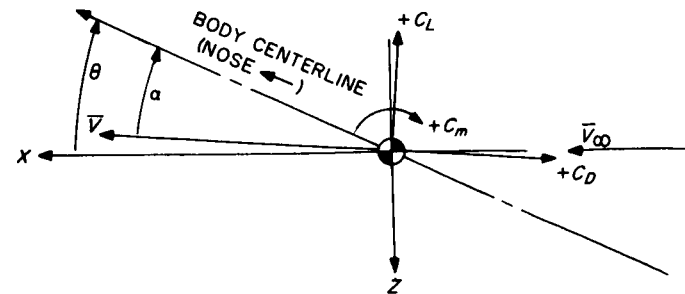


Fig. 1. Sign conventions

*Symbol definitions are included in the Nomenclature; sign conventions are shown in Fig. 1.

Multiplying through by θ' and integrating from the initial amplitude of oscillation, θ_0 , to the amplitude after a half cycle, $-(\theta_0 - \delta\theta)$, Eq. (7) becomes

$$\begin{aligned} \frac{\theta'^2}{2} \Big|_{\theta_0'}^{-(\theta_0 - \delta\theta)'} &= \frac{\rho A d}{2I} \int_{\theta_0}^{-(\theta_0 - \delta\theta)} \left\{ C_m(\theta) + [\alpha - \theta] \frac{dC_m(\theta)}{d\theta} \right. \\ &+ [C_{m_q} + C_{m_{\dot{\alpha}}}] \theta' d + C_{m_{\dot{\alpha}}} [\alpha' - \theta'] d \\ &\left. - \frac{2I}{\rho A d} \frac{\ddot{X}}{X^2} \theta' \right\} d\theta \end{aligned} \quad (8)$$

At the amplitudes, θ' is zero; therefore, the left side of the equation is equal to zero. This, in effect, is saying that there is a conservation of energy. In order to integrate the right side of Eq. (8), $[\alpha - \theta]$, $[\alpha' - \theta']$, \ddot{X}/X^2 , and θ' must be presented explicitly as functions of θ .

From Eq. (4c) and (4d),

$$\ddot{X} = -\frac{\rho \dot{X}^2 A}{2m} C_D(\alpha) + g_x \quad (9)$$

and

$$\ddot{Z} = -\frac{\rho \dot{X}^2 A}{2m} C_L(\alpha) + g_z \quad (10)$$

where C_D and C_L are, as denoted, functions of α .

From Eq. (4b) and (9),

$$\begin{aligned} \ddot{Z} &= -\ddot{X} [\theta - \alpha] - \dot{X} [\dot{\theta} - \dot{\alpha}] \\ &= \left[\frac{\rho \dot{X}^2 A}{2m} C_D(\alpha) - g_x \right] [\theta - \alpha] - \dot{X}^2 [\theta' - \alpha'] \end{aligned} \quad (11)$$

Combining Eq. (10) and (11),

$$\begin{aligned} [\alpha' - \theta'] &= \left[\frac{-\rho A}{2m} C_L(\alpha) + \frac{g_z}{X^2} \right] \\ &+ [\alpha - \theta] \left[\frac{\rho A}{2m} C_D(\alpha) - \frac{g_x}{X^2} \right] \end{aligned} \quad (12)$$

The second term on the right side of the equation is about two orders of magnitude smaller than the first and will be neglected. $[\alpha - \theta]$ at any θ can be obtained by a direct integration of Eq. (12):

$$[\alpha - \theta] = [\alpha - \theta]_0 + \int_{\theta_0}^{\theta} \left[\frac{-\rho A}{2m} C_L(\alpha) + \frac{g_z}{X^2} \right] \frac{d\theta}{\theta'} \quad (13)$$

Combining Eq. (9), (12), and (13) with Eq. (8), we have

$$\begin{aligned} 0 &= \frac{\rho A d}{2I} \int_{\theta_0}^{-(\theta_0 - \delta\theta)} \left\{ C_m(\theta) + [\alpha - \theta]_0 \right. \\ &- \int_{\theta_0}^{\theta} \left[\frac{\rho A}{2m} C_L(\alpha) - \frac{g_z}{X^2} \right] \frac{d\theta}{\theta'} \left. \right\} \frac{dC_m(\theta)}{d\theta} \\ &+ [C_{m_q} + C_{m_{\dot{\alpha}}}] \theta' d + C_{m_{\dot{\alpha}}} \left[\frac{-\rho A}{2m} C_L(\alpha) + \frac{g_z}{X^2} \right] d \\ &+ \frac{2I}{\rho A d} \left[\frac{\rho A}{2m} C_D(\alpha) - \frac{g_x}{X^2} \right] \theta' d \end{aligned} \quad (14)$$

To this point in the development, the only assumption employed was that the angle $[\alpha - \theta]$ was small. However, further assumptions are required in order to solve actual problems, as follows:

1. The lift and drag coefficients are assumed to be functions of θ directly,

$$C_L(\alpha) = C_L(\theta) \quad (15)$$

$$C_D(\alpha) = C_D(\theta) \quad (16)$$

In effect, this assumption says that the second terms in the Taylor-series expansions of lift and drag (see Eq. 6) will have a negligible influence on the solution of Eq. (14). In general, the lift and drag are second-order terms; a small error in them will lead to a negligible error in the final solution. For most physically probable situations, this error will be less than one-half of one percent.

2. The angular rate, θ' , is assumed to be a function only of the static pitching moment. The validity of this assumption can be seen from an inspection of the differential solution, Eq. (1). Aside from the static pitching moment, the only other term that affects the angular rate is the decay factor, λ . It enters into the frequency term, $-\rho A d C_{m_{\dot{\alpha}}}/2I + \lambda^2$, and modifies the amplitude which is proportional to θ' . In general this effect is small and can be neglected. From Eq. (6) and (13),

$$\theta' = \pm \left[\frac{\rho A d}{I} \int_{\theta_0}^{\theta} \left\{ C_m(\theta) + [\alpha - \theta] \frac{dC_m(\theta)}{d\theta} \right\} d\theta \right]^{1/2} \quad (17)$$

The proper sign to use can be obtained by differentiating Eq. (1). In the examples presented later, a positive initial amplitude will be assumed; correspondingly, the negative sign will be used. In general, the second term in the integral is negligible and can be neglected. If, however, it becomes important, this second term can be included by a process of

iteration, i.e., obtain the first order θ' from Eq. (17), excluding the second term, and evaluate $[\alpha - \theta]$ from Eq. (13) with this θ' . The results of Eq. (13) are then used to obtain a new θ' and the process is repeated until sufficient accuracy is obtained.

3. The \dot{X}^2 terms in the gravity expressions will be assumed constant; either the initial velocity V_∞ or some mean value for the integration can be used. Again, in general, gravity has a second-order effect and this assumption will result in a very small error.

Combining these assumptions into Eq. (14), reversing the limits of integration, splitting the $C_m(\theta)$ integral, and multiplying through by $[2m/\rho A]$, Eq. (14) becomes

$$\begin{aligned}
 0 = & -\frac{md}{I} \int_{-\theta_0}^{-(\theta_0-\delta\theta)} C_m(\theta) d\theta + \frac{md}{I} \int_{-\theta_0}^{+\theta_0} C_m(\theta) d\theta \\
 & + \frac{\rho Ad}{2I} \int_{-(\theta_0-\delta\theta)}^{+\theta_0} \left\{ \frac{2m}{\rho A} [\alpha - \theta]_0 \right. \\
 & - \left. \frac{dC_m(\theta)}{d\theta} \int_{+\theta_0}^{\theta} \left[C_L(\theta) - \frac{2mg_z}{\rho AV_\infty^2} \right] \frac{d\theta}{\theta'} \right\} d\theta \\
 & + \int_{-(\theta_0-\delta\theta)}^{+\theta_0} \left[C_D(\theta) - \frac{2mg_x}{\rho AV_\infty^2} \right] \theta' d\theta \\
 & + \frac{md^2}{I} \int_{-(\theta_0-\delta\theta)}^{+\theta_0} [C_{m_q} + C_{m_{\dot{\alpha}}}] \theta' d\theta \\
 & + \frac{md^2}{I} \int_{-(\theta_0-\delta\theta)}^{+\theta_0} C_{m_{\dot{\alpha}}} \left[-\frac{\rho A}{2m} C_L(\theta) + \frac{g_z}{V_\infty^2} \right] d\theta \quad (18)
 \end{aligned}$$

Equation (18) is the basic energy-integral equation. The formulation of this equation was originally presented in Ref. (3).

The first integral, quantitatively, is the Total Energy Defect. When there is no decay or divergence for the half cycle, $\delta\theta$ is zero and the integral is zero. This does not mean, however, that no decay or divergence occurred during each instant of the half cycle, but it does mean that the total effect for the half cycle, from all factors, is zero.

The second term is the Potential Energy Defect. This term will account for any hysteresis in the static pitching moment due to its being a double-valued function of θ . The ease by which a hysteresis is handled is one prime difference between the microscopic and macroscopic approaches. Intrinsic in the microscopic approach is the usual assumption that the static pitching moment is single-valued and, consequently, there is no hysteresis of the static pitching moment, nor is there a potential energy defect. This topic will be discussed later.

The third term is the Normal Motion Defect and is due to the fact that there is a difference between α and θ . A positive lift will induce a negative α deviation which, in turn, will reduce the potential energy due to the pitching moment. Another way to look at it is as follows. Consider a body with no lift at some angle of attack, $\bar{\alpha}$; since there is no lift, $\bar{\theta} = \bar{\alpha}$ (gravity and initial deviation are neglected). Suddenly, there is a gust of air down from above; this is analogous to a sharp upward movement of a body due to positive lift. The result is a slight negative deviation in α and, correspondingly, a decrease in the restoring moment and the potential energy due to this restoring moment. A positive lift slope tends to cause convergence.

The fourth term is the Deceleration Defect. The drag of the body causes a deceleration which, in turn, causes a continual reduction of the dynamic pressure. Since the dynamic pressure is a weighing factor in determining forces and moments from aerodynamic coefficients, a decrease in the dynamic pressure reduces the ability of the system to overcome the initial potential energy at θ_0 . A positive drag will tend to cause divergence.

The fifth and sixth terms are the Dynamic-Stability terms. The sixth term is generally two orders of magnitude smaller than the fifth term and is quite often neglected. Furthermore, experimentally, C_{m_q} and $C_{m_{\dot{\alpha}}}$ are inseparable; therefore, as far as extracting dynamic-stability data from experiments, the sixth term might be meaningless. Negative $[C_{m_q} + C_{m_{\dot{\alpha}}}]$ tends to cause convergence.

Particular solutions of Eq. (18) (excluding the last term), using several sets of hypothetical aerodynamic coefficients, were verified with exact six-degree-of-freedom computer solutions and were found to agree with differences generally less than two percent.

For a large class of problems, the gravity effects are small, $[\alpha - \theta]_0$ is negligible, and the sixth term can be ignored. In these cases, Eq. (18) is

$$\begin{aligned}
 0 = & -\frac{md}{I} \int_{-\theta_0}^{-(\theta_0-\delta\theta)} C_m(\theta) d\theta + \frac{md}{I} \int_{-\theta_0}^{+\theta_0} C_m(\theta) d\theta \\
 & - \frac{\rho Ad}{2I} \int_{-(\theta_0-\delta\theta)}^{+\theta_0} \frac{dC_m(\theta)}{d\theta} \int_{+\theta_0}^{\theta} \frac{C_L(\theta)}{\theta'} d\theta d\theta \\
 & + \int_{-(\theta_0-\delta\theta)}^{+\theta_0} C_D(\theta) \theta' d\theta \\
 & + \frac{md^2}{I} \int_{-(\theta_0-\delta\theta)}^{+\theta_0} [C_{m_q} + C_{m_{\dot{\alpha}}}] \theta' d\theta \quad (19)
 \end{aligned}$$

Also, for the majority of configurations the decay, $\delta\theta$, will be much smaller than the initial amplitude, θ_0 , and the lower limit of integration, $-(\theta_0 - \delta\theta)$, can be approximated by $-\theta_0$, further simplifying the solution.

One of the examples presented later shows that if first-order linear aerodynamics are considered, ($C_m(\alpha) = C_{m_\alpha}\alpha$, $C_D(\alpha) = C_{D_0}$, $C_L(\alpha) = C_{L_\alpha}\alpha$), and the decay is moderate such that $[-\delta\theta/\theta_0]$ can be approximated by the natural logarithm of $|\alpha_1/\alpha_0|$, the solution from Eq. (19) is equivalent to the solution from the differential equation,

Eq. (1), given below. The term, α_1 , is the angle-of-attack amplitude after a half cycle.

$$-\frac{\Omega}{\pi} \cdot \frac{4m}{\rho A} \cdot \ln \left| \frac{\alpha_1}{\alpha_0} \right| = C_{L_\alpha} - C_{D_0} - \frac{md^2}{I} [C_{m_q} + C_{m_{\dot{\alpha}}}] \quad (20)$$

The validity of approximating $[-\delta\theta/\theta_0]$ by $\ln |\alpha_1/\alpha_0|$ can be seen by expanding $\ln |\alpha_1/\alpha_0|$ in a series and noting that for no initial normal motion, $\theta_0 = \alpha_0$.

III. EXAMPLES

A. Local and Effective Constant Dynamic-Stability Coefficients

For a specified decay the value of each of the terms in the energy-integral equation is dependent only upon θ and can be considered a constant. Equation (19) can, therefore, be written as follows:

$$0 = K_0 + K_1 + K_2 + K_3 + \frac{md^2}{I} \int_{-(\theta_0 - \delta\theta)}^{+\theta_0} [C_{m_q} + C_{m_{\dot{\alpha}}}] \theta' d\theta$$

or

$$K = \int_{-(\theta_0 - \delta\theta)}^{+\theta_0} [C_{m_q} + C_{m_{\dot{\alpha}}}] \theta' d\theta$$

As indicated before, $[C_{m_q} + C_{m_{\dot{\alpha}}}]$ is an arbitrary function and for future reference will be denoted as the "local" dynamic stability coefficient. It is desirable to define an "effective constant" (EFF) dynamic-stability coefficient which will yield the same energy defect for the half cycle, i.e.,

$$[C_{m_q} + C_{m_{\dot{\alpha}}}]_{EFF} \int_{-(\theta_0 - \delta\theta)}^{+\theta_0} \theta' d\theta = \int_{-(\theta_0 - \delta\theta)}^{+\theta_0} [C_{m_q} + C_{m_{\dot{\alpha}}}]_{Local} \theta' d\theta = K \quad (21)$$

This coefficient is valuable because in the reduction of experimental free-flight and free-oscillation data, it is the effective constant coefficient that is obtained.

The local dynamic stability coefficient, right hand side of Eq. (21), could be a function of anything, θ , θ' , θ_0 , etc.; only the equality of Eq. (21) must be obeyed. Figure 2 shows two examples where the local dynamic-stability coefficients are functions of the angle of attack. Cases A and B depict local values of $[C_{m_q} + C_{m_{\dot{\alpha}}}]$ of the parabolic form $[C_{m_q} + C_{m_{\dot{\alpha}}}]_0 + K\alpha^2$. The Case A local value increases (negatively) with angle of attack from -0.3 at 0 deg to -0.7 at 25 deg. Integrating the local curve over the angle-of-attack region -25 to 25 deg as indicated in Eq. (21) for an amplitude of 25 deg results in an effective constant dynamic-stability coefficient of -0.4 (assuming a linear static pitching moment and a small decay). Similarly, effective constant values were obtained at all the other amplitudes for both Cases A and B; Case B decreased (negatively) as much as Case A increased (negatively). Both results are shown as the dashed curves in Fig. 3. Although the difference between these two local curves is substantial, the effective curves do not show this large difference. The change in the local curve is greatly attenuated when converted to the effective constant curve. The reason becomes obvious when it is realized that θ' is a weighing factor in the integration, and θ' looks sinusoidal with its largest value when $\alpha = 0$. The local

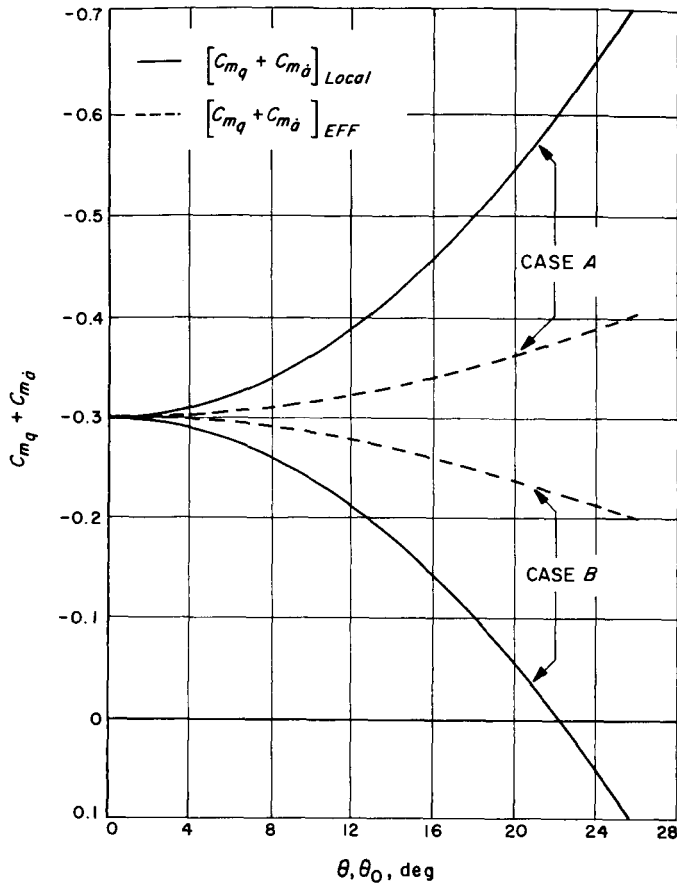


Fig. 2. Local and corresponding effective constant dynamic-stability curves

dynamic stability values near the amplitude play a small part in determining the effective constant value.

The solution for the effective constant dynamic-stability coefficient from a local dynamic-stability coefficient of the form

$$[C_{m_q} + C_{m_{\dot{\alpha}}}]_{Local} = a + b|\theta| + c\theta^2 + d|\theta|^3$$

is

$$[C_{m_q} + C_{m_{\dot{\alpha}}}]_{EFF} = a + \frac{4}{3} \pi b |\theta_0| + \frac{1}{4} c \theta_0^2 + \frac{8}{15} \pi d |\theta_0|^3$$

(assuming a linear pitching moment and a small decay). Figure 3 contains the experimental effective constant dynamic-stability data from a typical sting-fixed free-oscillation test (Ref. 4). A cubic curve fit of the data from 0 to 17 deg was made (dashed line); from this, the local curve which would yield the effective constant value at each amplitude was determined from the above expression. The local curve is shown as the dash-dot line. Another cubic fit of the experimental data was made

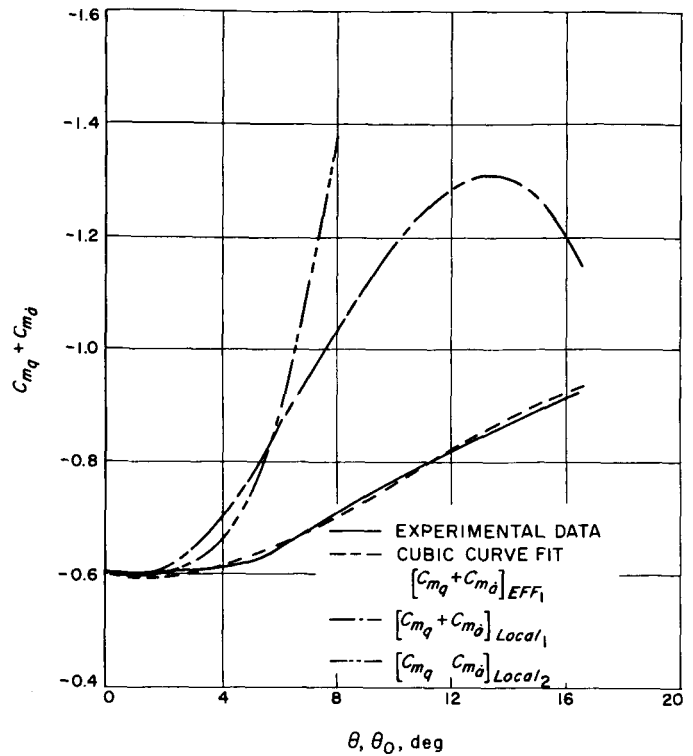


Fig. 3. Typical test data

from 0 to 8 deg, and again in the corresponding local curve was determined (dash-dot-dot line). The curve fit agreed very well with the experimental data; the difference being so small as to not be perceptible on the plot. Although the two effective constant curve fits deviate only slightly, the local curves differ greatly. It should be noted that the difference between the two curve fits is about the same magnitude as the scatter of the experimental data. Even the slightest wiggle in the effective constant curve is greatly amplified when converted to a local curve.

Similar comparisons can be made where the local dynamic stability is generated according to some other dependence. For instance, consider the dynamic stability coefficient to be of the form

$$[C_{m_q} + C_{m_{\dot{\alpha}}}]_{Local} = [C_{m_q} + C_{m_{\dot{\alpha}}}]_0 + k \theta'$$

The corresponding effective dynamic stability from Eq. (21) with the assumption of a linear pitching moment is

$$[C_{m_q} + C_{m_{\dot{\alpha}}}]_{EFF} = [C_{m_q} + C_{m_{\dot{\alpha}}}]_0 + \frac{8k}{3\pi} \theta'_{max}$$

where θ'_{max} is a function of the amplitude, θ_0 , as indicated by Eq. (17); therefore, the effective dynamic-stability coefficient is also a function of the amplitude. Mathematically then, what on the surface would appear to be

an amplitude effect could, in reality, be an angular velocity effect.

B. Nonlinear Aerodynamics

The energy approach has obvious applications for configurations with nonlinear static aerodynamics. For instance, consider the class of bodies whose aerodynamic coefficients can be expressed as follows:

$$\begin{aligned}
 C_L(\alpha) &= C_{L\alpha} \alpha + c_1 \alpha^3 \\
 C_D(\alpha) &= C_{D0} + c_2 \alpha^2 + c_3 \alpha^4 \\
 C_m(\alpha) &= C_{m\alpha} \alpha
 \end{aligned}$$

where the coefficients of α^p are constants. Assuming that $\delta\theta \ll \theta_0$, a closed form solution of Eq. (19) can be obtained with these coefficients.

The Total Energy Defect is

$$-\frac{md}{I} \int_{-\theta_0}^{-(\theta_0 - \delta\theta)} C_{m\alpha} \theta d\theta = -\frac{md}{I} C_{m\alpha} \theta_0 \cdot \delta\theta \tag{22}$$

The Potential Energy Defect is

$$\frac{md}{I} \int_{-\theta_0}^{+\theta_0} C_{m\alpha} \theta d\theta = 0$$

The Normal Motion Defect is

$$\begin{aligned}
 -\frac{\rho A d}{2I} \int_{-\theta_0}^{+\theta_0} C_{m\alpha} \int_{+\theta_0}^{\theta} \frac{C_{L\alpha} \theta + c_1 \theta^3}{-\Omega [\theta_0^2 - \theta^2]^{1/2}} d\theta d\theta \\
 = - [C_{L\alpha} + \frac{3}{4} c_1 \theta_0^2] \frac{\pi}{2} \theta_0^2 \Omega \tag{23}
 \end{aligned}$$

The Deceleration Defect is

$$\begin{aligned}
 -\int_{-\theta_0}^{+\theta_0} -\Omega [C_{D0} + c_2 \theta^2 + c_3 \theta^4] [\theta_0^2 - \theta^2]^{1/2} d\theta \\
 = [C_{D0} + \frac{1}{4} c_2 \theta_0^2 + \frac{1}{8} c_3 \theta_0^4] \frac{\pi}{2} \theta_0^2 \Omega \tag{24}
 \end{aligned}$$

The Dynamic Stability Defect is

$$\begin{aligned}
 \frac{md^2}{I} \int_{-\theta_0}^{+\theta_0} -\Omega [C_{m_q} + C_{m_{\dot{\alpha}}}]_{EFF} [\theta_0^2 - \theta^2]^{1/2} d\theta \\
 = \frac{md^2}{I} [C_{m_q} + C_{m_{\dot{\alpha}}}] \frac{\pi}{2} \theta_0^2 \Omega \tag{25}
 \end{aligned}$$

Combining the terms, dividing through by $\pi/2 \cdot \theta_0^2 \Omega$, and noting that

$$\frac{md}{I} C_{m\alpha} = -\frac{2m}{\rho A} \Omega^2$$

the following solution is obtained:

$$\begin{aligned}
 \frac{\Omega}{\pi} \cdot \frac{4m}{\rho A} \cdot \frac{\delta\theta}{\theta_0} &= [C_{L\alpha} + \frac{3}{4} c_1 \theta_0^2] - [C_{D0} + \frac{1}{4} c_2 \theta_0^2 \\
 &+ \frac{1}{8} c_3 \theta_0^4] - \frac{md^2}{I} [C_{m_q} + C_{m_{\dot{\alpha}}}]_{EFF} \tag{26}
 \end{aligned}$$

Note that if c_1 , c_2 , and c_3 are zero and $[-\delta\theta/\theta_0] = \ln |\alpha_1/\alpha_0|$, the problem reduces to the case of first-order linear aerodynamics and Eq. (26) reduces to Eq. (20). This solution can be used for the reduction of free-flight data by obtaining a mean $\delta\theta/\theta_0$ from a plot of the logarithm of the amplitude vs. X . Experience has shown (Ref. 5) that the logarithm of the amplitude data from a flight is usually quite linear. Occasionally, when the flight is long or there is a large amplitude effect, a curve in the logarithm amplitude plot is observed. In these cases, the data are separated into mean linear sections and a dynamic-stability coefficient is obtained for each section.

In general, the Normal Motion Defect term is the most difficult to evaluate for an arbitrary θ' because θ' appears in the denominator, complicating the integration. However, in many instances, simplifying the form of θ' to facilitate evaluation of this term will add only small errors in the total result. For instance, if $C_m(\alpha)$ is of the form $C_{m\alpha} \alpha + k_1 \alpha^3 + k_2 \alpha^5$, it is impossible to obtain a closed-form solution for the Normal Motion Defect using the lift curve of the previous example. However, an effective $C_{m\alpha}$ which would yield the same kinetic energy at θ equal to zero can be obtained from Eq. (17), and the Normal Motion Defect evaluated with it; if this defect is small or moderate in comparison to the total, this approximation will prove very satisfactory.

Although linear pitching moments are the simplest to use, others can certainly be considered. For instance, Ref. 3 contains a general solution for a pitching moment of the form $C_m(\alpha) = M \sin [r\alpha]$, where M and r are constants. In addition, it presents a closed-form solution for aerodynamics of the following form:

$$\text{axial-force coefficient} = A \cos \alpha$$

$$\text{normal-force coefficient} = N \sin \alpha$$

$$\text{pitching-moment coefficient} = M \sin \alpha$$

where A , N , and M are constants. These solutions are particularly valuable for high-amplitude oscillations.

C. Nonsymmetric Bodies

Another area where this approach could prove valuable is in the investigation of nonsymmetric or lifting bodies. Eq. (14) can be written in a more general way by changing the upper limit of integration from $-(\theta_0 - \delta\theta)$ to $-(\theta_1 - \delta\theta)$, where $-\theta_1$ is the negative amplitude of a conservative system (no lift, drag, or dynamic stability), and $-(\theta_1 - \delta\theta)$ is the negative amplitude of a decaying system. In a conservative system a body will oscillate from $+\theta_0$ to $-\theta_1$ to $+\theta_0$, etc., where the potential energy at $-\theta_1$ equals that at $+\theta_0$. Mathematically, $-\theta_1$ is the lower limit required to make the Potential Energy Defect integral equal to zero (assuming no static pitching moment hysteresis), i.e.,

$$\int_{-\theta_1}^{+\theta_0} C_m(\theta) d\theta = 0 \tag{27}$$

The equations can be modified to account for nonsymmetric aerodynamics by merely changing the limits of integration as indicated above. Equation (19) then becomes

$$\begin{aligned} 0 = & -\frac{md}{I} \int_{-\theta_1}^{-(\theta_1 - \delta\theta)} C_m(\theta) d\theta + \frac{md}{I} \int_{-\theta_1}^{+\theta_0} C_m(\theta) d\theta \\ & - \frac{\rho A d}{2I} \int_{-(\theta_1 - \delta\theta)}^{+\theta_0} \frac{dC_m(\theta)}{d\theta} \int_{\theta_0}^{\theta} \frac{C_L(\theta')}{\theta'} d\theta' d\theta \\ & + \int_{-(\theta_1 - \delta\theta)}^{+\theta_0} C_D(\theta) \theta' d\theta \\ & + \frac{md^2}{I} \int_{-(\theta_1 - \delta\theta)}^{+\theta_0} [C_{m_q} + C_{m_{\dot{\alpha}}}] \theta' d\theta \end{aligned} \tag{28}$$

As an example, consider a configuration which has first-order linear aerodynamics but also has an offset center of gravity; the corresponding aerodynamic coefficients for this body would be

$$\begin{aligned} C_m(\alpha) &= C_{m_0} + C_{m_\alpha} \alpha \\ C_L(\alpha) &= C_{L_0} + C_{L_\alpha} \alpha \\ C_D(\alpha) &= C_{D_0} \end{aligned}$$

where C_{m_0} and C_{L_0} are the pitching-moment coefficient and lift-coefficient offsets. If one goes through the lengthy process of solving Eq. (28) with these coefficients, the following relatively simple solution, for the decay over the first half cycle, is obtained:

$$\begin{aligned} \frac{\Omega}{\pi} \cdot \frac{4m}{\rho A} \cdot \frac{\theta_0 + 3k}{[\theta_0 + k]^2} \cdot \delta\theta &= C_{L_\alpha} - C_{D_0} \\ & - \frac{md^2}{I} [C_{m_q} + C_{m_{\dot{\alpha}}}]_{EFF} + 2 \left[\frac{C_{L_0} - k C_{L_\alpha}}{\theta_0 + k} \right] \end{aligned} \tag{29}$$

where

$$k = \frac{C_{m_0}}{C_{m_\alpha}}$$

Note, if there is no offset, k is zero and C_{L_0} is zero and the above equation reduces to the linear aerodynamic solution, Eq. (20).

The same solution, Eq. (29), can be used to obtain the decay for the second half cycle by changing the starting amplitude from θ_0 to $(\theta_1 - \delta\theta)$, and replacing C_{m_0} and C_{L_0} with the negatives of the values used for the first half cycle. In this example, $[\theta_1 - \delta\theta]$ equals $[\theta_0 + 2k - \delta\theta]$; θ_1 was obtained by solving for the lower limit of Eq. (27). Denoting $\delta\theta_1$ as the decay for the first half cycle, the decay over the second half cycle, $\delta\theta_2$, is

$$\begin{aligned} \frac{\Omega}{\pi} \cdot \frac{4m}{\rho A} \cdot \frac{\theta_0 + 5k - \delta\theta_1}{[\theta_0 + 3k - \delta\theta_1]^2} \delta\theta_2 &= C_{L_\alpha} - C_{D_0} \\ & - \frac{md^2}{I} [C_{m_q} + C_{m_{\dot{\alpha}}}]_{EFF} + 2 \left[\frac{-C_{L_0} - k C_{L_\alpha}}{\theta_0 + 3k - \delta\theta_1} \right] \end{aligned} \tag{30}$$

D. Static Pitching-Moment Hysteresis

The previous solutions were obtained within the framework of the differential approach, assuming that the dynamic stability coefficient is a function of the local conditions and that all damping not accounted for specifically by the lift and drag must be due to the dynamic stability. However, there is some question about the completeness of this analytic model. From a total system energy point of view, it is apparent that the pitching moment is the principal factor. As a matter of fact, for 1-in.-D free-flight cones designed to accentuate dynamic stability, the ratio of the energy dissipated due to the dynamic stability coefficient after a quarter cycle to the potential energy at the beginning of the cycle due to the pitching moment was four percent, or eight percent for a half cycle. The combined lift and drag accounted for an additional two percent for the half cycle. According to the present flow model of static coefficients, the pitching moment of a cone is symmetrical with angle of attack (C_m is a single-valued function of α) and, consequently, the Potential Energy Defect term of the energy-integral equation is zero. However, consider the following possibility. As the cone oscillates from $\theta = 0$ to say θ_* , separation occurs on the lee side of the cone. (Experimental boundary-layer investigations and theoretical studies by Moore (Ref. 6) indicate this will occur somewhat before reaching the cone semivertex angle). The body continues to oscillate to the amplitude, θ_0 , and

returns to θ_* still in the separated mode, but instead of re-attaching at θ_* it re-attached at $(\theta_* - \epsilon)$. During the separated mode, the pressure on the aft portion of the cone on the lee side will be greater than if the flow were attached, and the pitching moment will be more positive than for the attached flow. Figure 4 contains a hypothetical pitching-moment curve exhibiting this condition. A body at θ_0 will travel down the A curve and on to a B curve. However, since the area under the A curve is less than the area under the B curve, there will not be enough kinetic energy developed at $\theta = 0$ to pitch the model to $-\theta_0$ and a decay will result; analytically, this result is obtained by integrating the Potential Energy Defect term with the hypothetical pitching moment. Since the ratio of the area between the A and B curves to the area under the A curve is the Potential Energy Defect, even a one percent defect in the case of the 1-in.-D dynamic-stability cone would account for 10 percent of the over-all amplitude decay.

Another example where this type of flow hysteresis could develop is the following. Consider an entry vehicle, near peak heating, oscillating at perhaps 3 cps. Three times every second, the ablation surface on each side of the vehicle goes through a heating cycle. If the surface is cooled sufficiently while it is in the lee phase of the cycle, there will be a time lag between the heat pulse and ablation when it enters the windward phase of the cycle. Consequently, there would be a delayed alteration of the flow field due to the addition of ablation products on the increasing angle stroke, and a persistence of ablation after the heat pulse during the decreasing stroke. The result then would be a hysteresis of the pitching moment causing a decay or divergence, depending on how ablation affects the flow. If, hypothetically, the affect of ablation is to change the effective shape of the body such that the aerodynamic restoring moment is greater, then the result would be just opposite to that of the previous example, and a decrease in the decay would occur.

One could ask what would be the consequences of lumping this kind of hysteresis damping with an effective dynamic stability coefficient. To answer this question, consider the problem of using test information from a small test body to predict the motion of a much larger

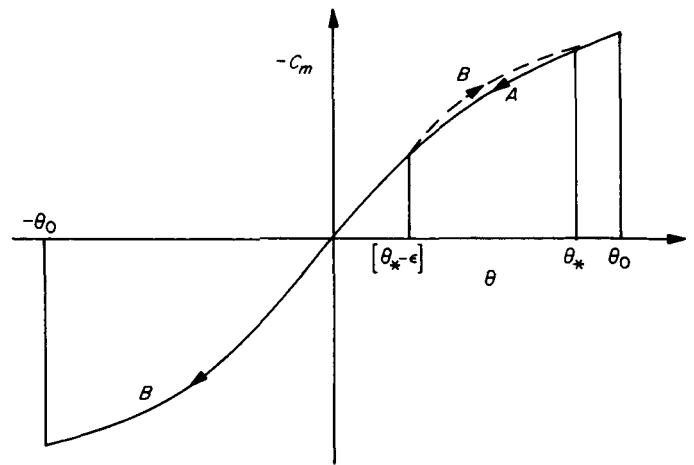


Fig. 4. Hypothetical pitching moment due to separation hysteresis

vehicle. For the discussion assume that the body nominally has linear aerodynamics but also exhibits a static pitching-moment hysteresis. The ratio of decay to initial amplitude is

$$\frac{\delta\theta}{\theta_0} = -\frac{1}{\theta_0^2} \int_{-\theta_0}^{+\theta_0} C_m(\theta) d\theta + \frac{\pi}{\Omega} \cdot \frac{\rho A}{4m} \left\{ C_{L\alpha} - C_{D_0} - \frac{md^2}{I} [C_{m_q} + C_{m_{\dot{\alpha}}}]_{EFF} \right\} \quad (31)$$

If the media density is the same, the influence of the static and dynamic coefficients is determined by the factors A/m , $1/\Omega$, and md^2/I . It is difficult to say how these terms will vary from the test body to the flight vehicle without considering a specific case. However, experience with free-flight test bodies indicates that usually all these factors tend to decrease as the body size is increased from the wind-tunnel test model to the actual flight vehicle. For this situation it is obvious that the Potential Energy Defect will contribute more, percentage wise, to the total decay as the body size increases, and a prediction of decay using an effective dynamic stability coefficient, which includes the effects of hysteresis, will be in error. In short, the causes of motion decay (or divergence) must be properly evaluated in order to permit proper scaling; this includes lift, drag, and pitching moment, as well as dynamic stability.

IV. CONCLUSION

This Report presented the idea of viewing dynamic stability from a macroscopic or energy-integral point of view. Several examples were presented which demonstrate the application of this approach to problems not generally solvable with the differential approach, including solutions with nonlinear static and dynamic coefficients and lifting bodies. It is also suggested that there are factors that can cause an amplitude decay which are not being accounted for in the differential approach and can be accounted for in the energy-integral approach,

e.g., double-valued pitching moments. It is further suggested that lumping a hysteresis effect into an effective dynamic-stability coefficient could result in erroneous results when experimental data are used to predict the motion of actual flight vehicles.

It is felt that this approach offers great latitude, as an analytic tool, for investigating different forms of the dynamic-stability coefficient and different hypotheses of the decay mechanism.

NOMENCLATURE

C_m, C_L, C_D	pitching moment, lift, and drag coefficients; moment/ $\frac{1}{2} \rho V^2 A d$, lift/ $\frac{1}{2} \rho V^2 A$, drag/ $\frac{1}{2} \rho V^2 A$; these coefficients are functions of α : $C_m = C_m(\alpha)$, $C_L = C_L(\alpha)$, $C_D = C_D(\alpha)$
$C_{m\dot{\alpha}}, C_{L\dot{\alpha}}, C_{D0}$	linear pitching-moment coefficient slope (rad^{-1}), linear lift-coefficient slope (rad^{-1}), and drag coefficient at $\alpha = 0$, respectively
$[C_{m\dot{q}} + C_{m\dot{\alpha}}]$	dynamic stability coefficient, nominally: $\left[\frac{\partial C_m}{\partial \left(\frac{\dot{\theta} d}{V} \right)} + \frac{\partial C_m}{\partial \left(\frac{\dot{\alpha} d}{V} \right)} \right]$
d, A, I, m	body reference length (ft), reference area (ft^2), transverse moment of inertia (slug-ft^2), and mass (slug), respectively
EFF	effective constant
g_x, g_z	gravitational accelerations in the X and Z directions, respectively, ft/sec^2
\bar{V}	velocity of the body center of mass; $V = \bar{V} $, ft/sec
\bar{V}_∞	initial free-stream velocity
X	body position relative to the media measured in the initial free-stream velocity direction, ft
α	angle of attack; angle between \bar{V} and the model centerline, rad
α_0	initial angle-of-attack amplitude, rad
$\delta\theta$	decay for a half cycle, rad
θ	angle between the initial free-stream velocity, \bar{V}_∞ , and the body centerline, rad
θ_0	initial amplitude of oscillation, rad

NOMENCLATURE (Cont'd)

ρ	media density, slug/ft ³
Ω	frequency of oscillation per distance, X , traveled, rad/ft; for a linear pitching moment, $\Omega = \left[\frac{-\rho A d}{2I} C_{m\alpha} \right]^{1/2}$
$(\dot{\quad}), (\ddot{\quad})$	first and second derivatives of () with respect to time
$(\dot{\quad}), (\ddot{\quad})'$	first and second derivatives of () with respect to X

REFERENCES

1. Nicolaides, John D., "On the Free-Flight Motion of Missiles Having Slight Configurational Asymmetries," *Ballistic Research Laboratory Report No. 858*, Aberdeen Proving Ground, Md., June, 1953.
2. Murphy, Jr., Charles H., "The Prediction of Nonlinear Pitching and Yawing Motion of Symmetric Missiles," *Journal of the Aeronautical Sciences*, Vol. 24, No. 7, pp. 473-479, July, 1957.
3. Jaffe, Peter, *Obtaining Free-Flight Dynamic Damping of an Axially Symmetric Body (At All Angles of Attack) in a Conventional Wind Tunnel*, Technical Report No. 32-544, Jet Propulsion Laboratory, Pasadena, California, January, 1964.
4. Prislín, Robert, and Jaffe, Peter, "Dynamic Stability Research," *JPL Space Programs Summary No. 37-32, Vol. IV*, April 30, 1965.
5. Jaffe, Peter, and Prislín, Robert H., "Effect of Boundary-Layer Transition on Dynamic Stability over Large Amplitudes of Oscillation," *AIAA Paper No. 64-427*, June, 1964.
6. Moore, Franklin K., "Laminar Boundary-Layer on Cone in Supersonic Flow at Large Angle of Attack," *NACA TN 2844*, November, 1952.